

Advanced modelling of structures and properties of crystalline, nanocrystalline and amorphous nitrogen-based materials

Jiri Houska

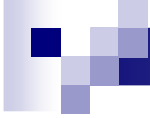
Department of Physics, University of West Bohemia, Czech Republic



► **FACULTY
OF APPLIED SCIENCES
UNIVERSITY
OF WEST BOHEMIA**

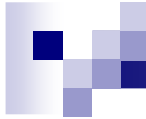


**DEPARTMENT
OF PHYSICS**



Objectives

- Review usefulness (range of phenomena captured) of various simulation techniques
 - different levels of theory
 - different simulation protocols used
- Show examples for different classes of novel materials
 - crystalline
 - nanocrystalline
 - amorphous



Outline

	DFT (Ab-initio)	Empirical potentials
Properties		
Liquid-quench		
Atom by atom dep.		

Outline

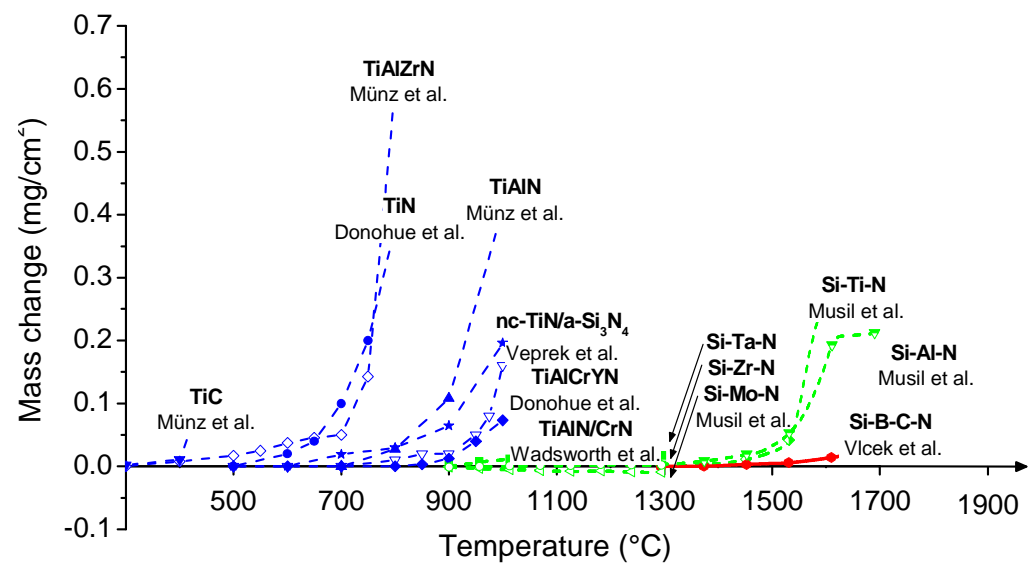
	DFT (Ab-initio)	Empirical potentials
Properties	3. crystalline (Ti/Cr)N+Si,C	
Liquid- quench	1. amorphous (dense) SiBCN	2. nanocomposite TiN+SiN
Atom by atom dep.		4. amorphous (voids) SiNH

1. Amorphous SiBCN

	DFT (Ab-initio)	Empirical potentials
Properties	3. crystalline (Ti/Cr)N+Si,C	
Liquid- quench	1. amorphous (dense) SiBCN	2. nanocomposite TiN+SiN
Atom by atom dep.		4. amorphous (voids) SiNH

Motivation (a-SiBCN)

- Superior high temperature behavior
 - amorphous structure stable up to a 1700 °C limit
 - extremely high oxidation resistance in air above 1500 °C
- Stable functional properties
 - high hardness (up to 35 GPa)
 - transparency ($k_{550\text{nm}} = 2 \times 10^{-4}$)
 - low thermal cond. ($1.3 \text{ Wm}^{-1}\text{K}^{-1}$)
 - low compressive stress (1 GPa)
- Applications for high T
 - protective coatings
 - sensor components
 - microelectronics
 - fibres for composites
- See also
 - A1-2-7 (P.Zeman, Tuesday 15:30, Sunrise)
 - AP-3 (P.Steidl, Thursday poster)



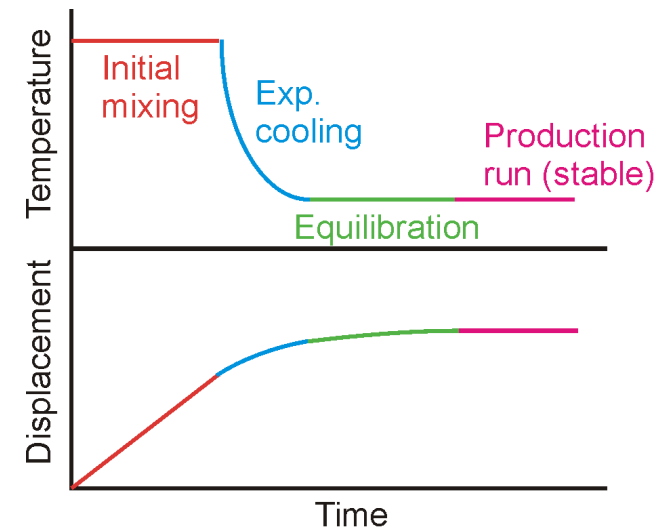
Methodology needed (a-SiBCN)

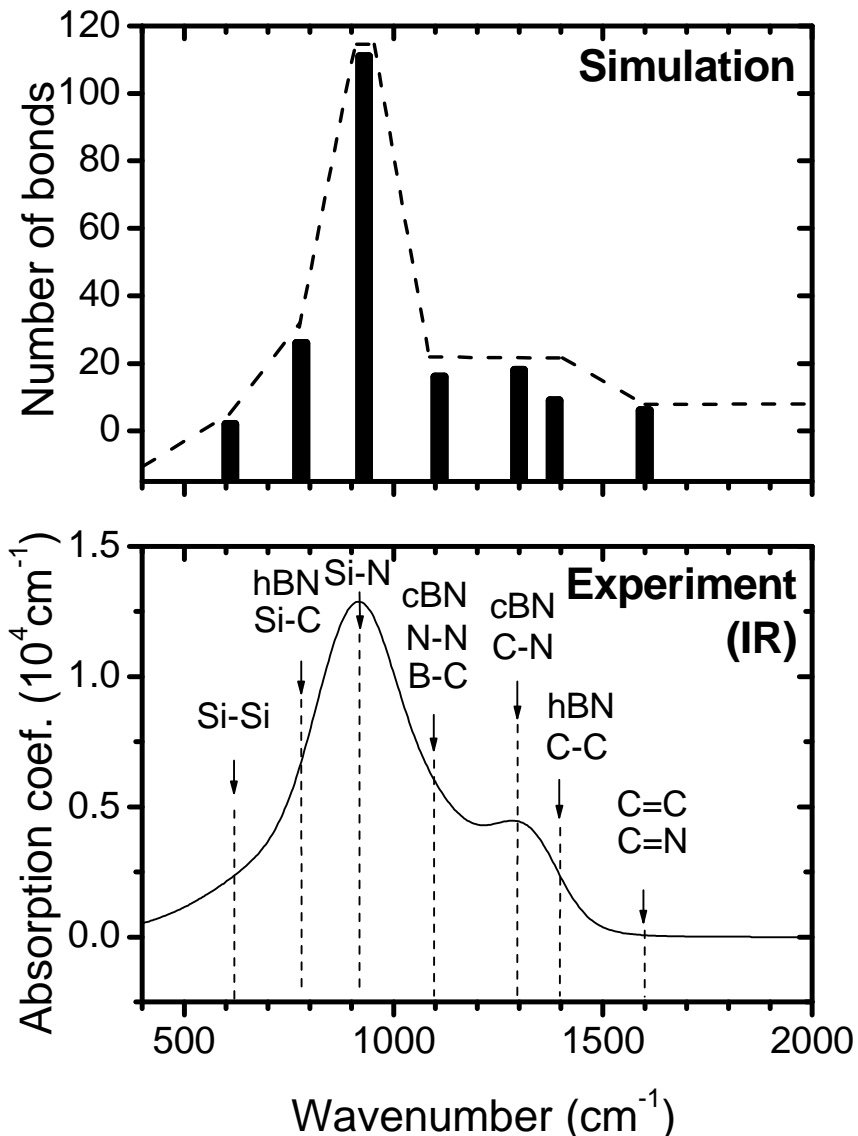
- **Energy (\Rightarrow forces for molecular dynamics)**

- DFT: implemented in the CPMD code
- atom cores and inner electron shells: Goedecker-type pseudopotentials
- valence electrons wavefunction: Kohn-Sham (Schrödinger-like) equations

- **Molecular-dynamics simulation protocol in order to predict material structure**

- Liquid-quench algorithm captures material formation conditions arising from rapid cooling of the localized melt around sites of energetic ion impact

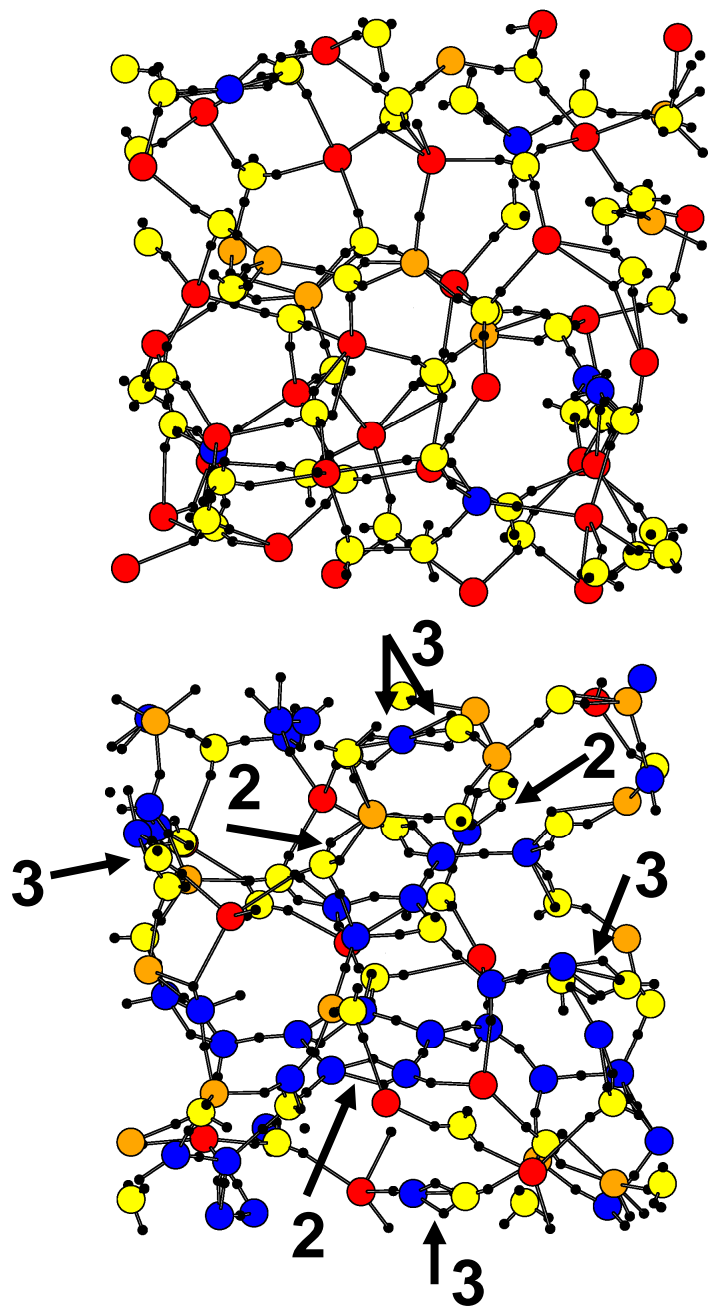




Bonding statistics of Si-B-C-N materials: experimental verification

Composition $\text{Si}_{32}\text{B}_8\text{C}_6\text{N}_{54}$ (Ar, H, O neglected)

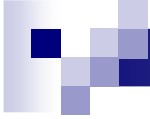
- Example of hard, transparent, thermally stable composition
- Quantitative agreement with experiment
(no oscillator strengths, single BN bonds in both c-BN and h-BN peaks)



Bonding statistics of Si-B-C-N materials: effect of composition

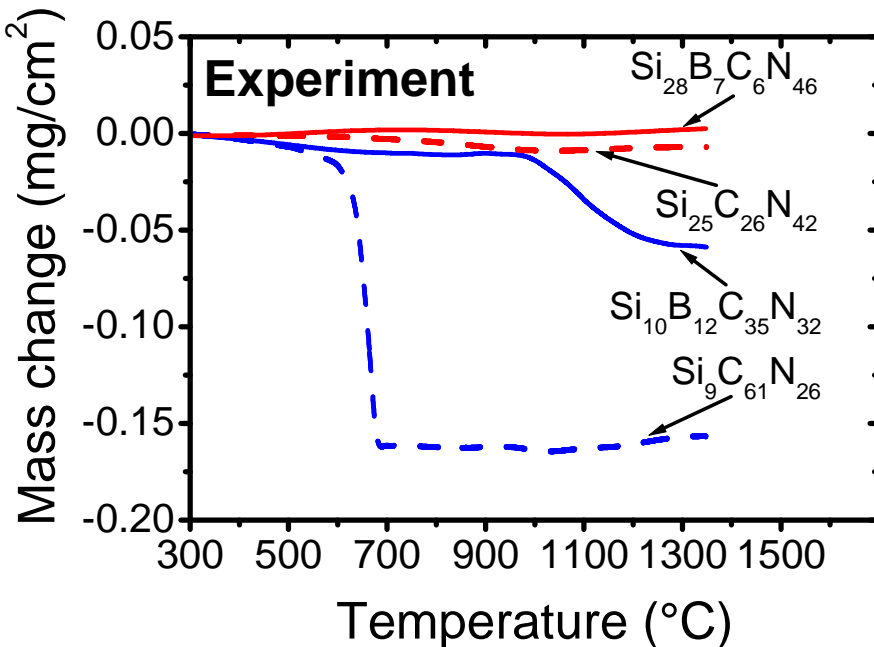
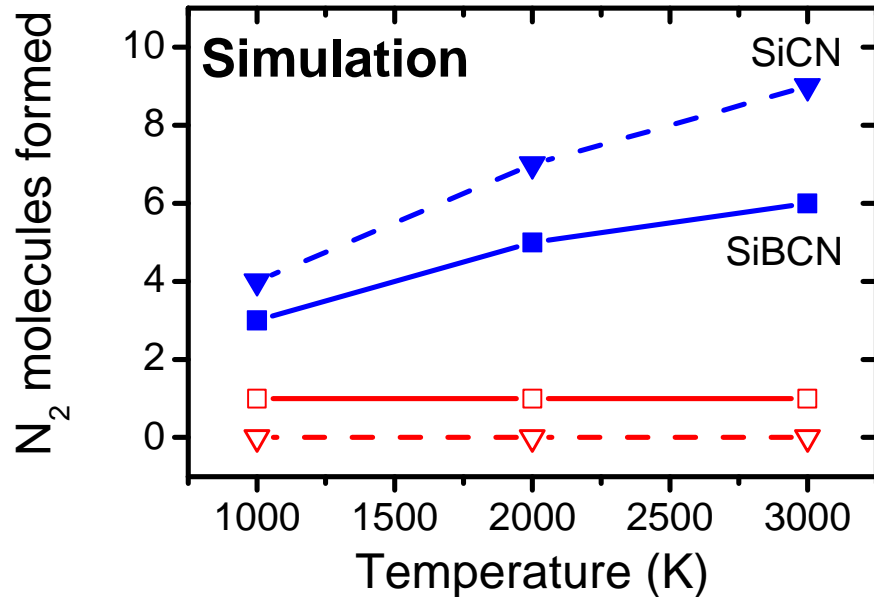
Si: ●, B: ○, C: ●, N: ●,
2 valence electrons: —●—

- $\text{Si}_{32}\text{B}_8\text{C}_6\text{N}_{54}$
Single Si-N bonds
⇒ high coordination
- $\text{Si}_{11}\text{B}_{14}\text{C}_{39}\text{N}_{36}$
Double C=N, C=C and
B=N, and triple C≡N
bonds
⇒ low coordination



Methodology needed - thermal stability (a-SiBCN)

- 1) Temperature-dependence of formation of N₂ molecules
- 2) Temperature dependence of bond lifetimes
- 3) Bonding statistics (using known relative stability of various bond types)



Temperature stability of Si-(B)-C-N materials: from N_2 formation

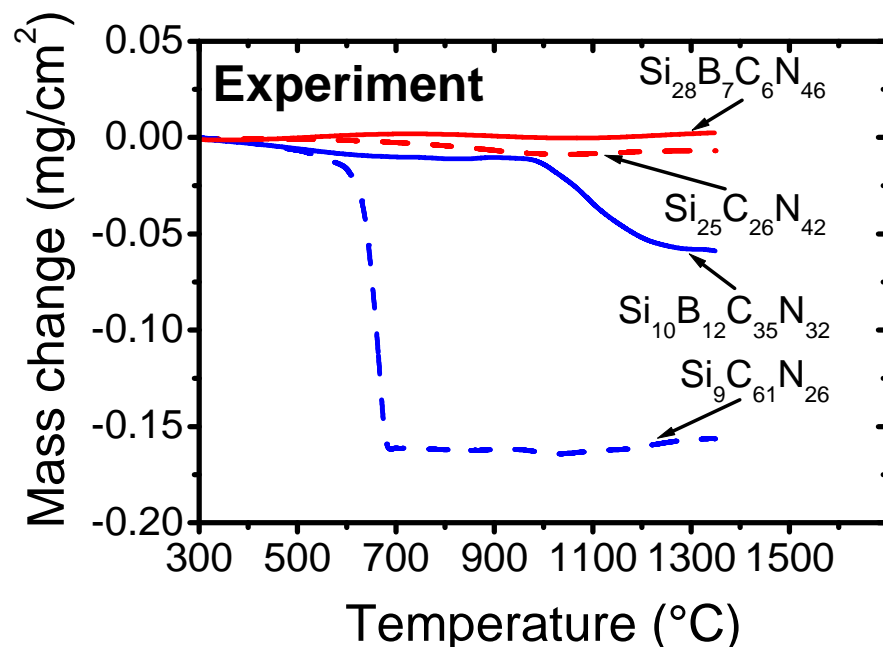
Simulated compositions

$\text{Si}_{39}\text{B}_{14}\text{C}_{11}\text{N}_{44}$, $\text{Si}_{53}\text{C}_{11}\text{N}_{44}$,
 $\text{Si}_{11}\text{B}_{14}\text{C}_{39}\text{N}_{44}$, $\text{Si}_{11}\text{C}_{53}\text{N}_{44}$

- Decomposition reactions
 $\text{Si}_3\text{N}_4 + 3\text{C} \rightarrow 3\text{SiC} + 2\text{N}_2$
and $\text{Si}_3\text{N}_4 \rightarrow 3\text{Si} + 2\text{N}_2$
 \Rightarrow mass loss due to formation of N_2 molecules
- Less N_2 molecules formed at (1) higher **Si/C** ratio and (2) **B** addition

Simulation

bond type	bond lifetime 1000 K (%)	bond lifetime 2400 K (%)
low Si/C ($Si_{11}B_{14}C_{39}N_{36}$)		
Si-N	46	33
B-N	53	45
C-N	48	40
high Si/C ($Si_{32}B_8C_6N_{54}$)		
Si-N	82	59
B-N	89	70
C-N	96	68

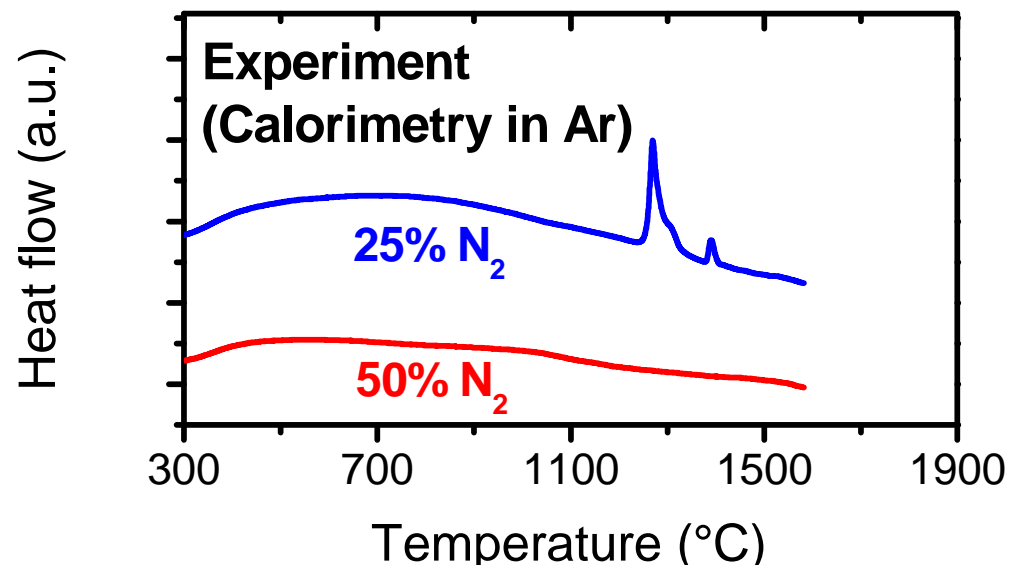
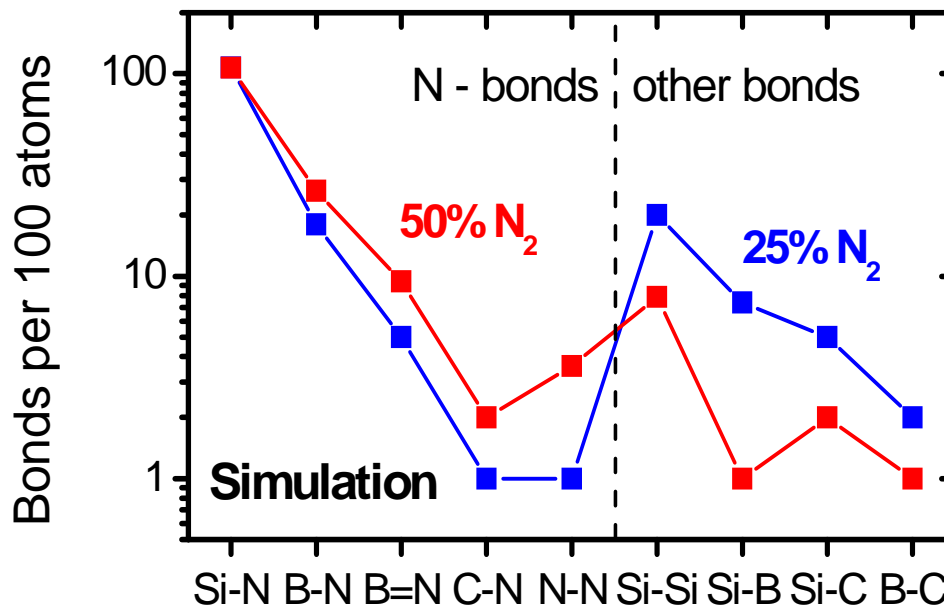
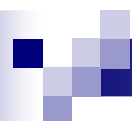


Temperature stability of Si-(B)-C-N materials: from bond lifetimes

Simulated compositions

$Si_{32}B_8C_6N_{54}$, $Si_{11}B_{14}C_{39}N_{36}$

- Higher bond lifetimes in compositions with higher **Si/C** ⇒ more stable network ⇒ limited diffusion ⇒ decomposition reactions shifted to higher T ⇒ improved thermal stability



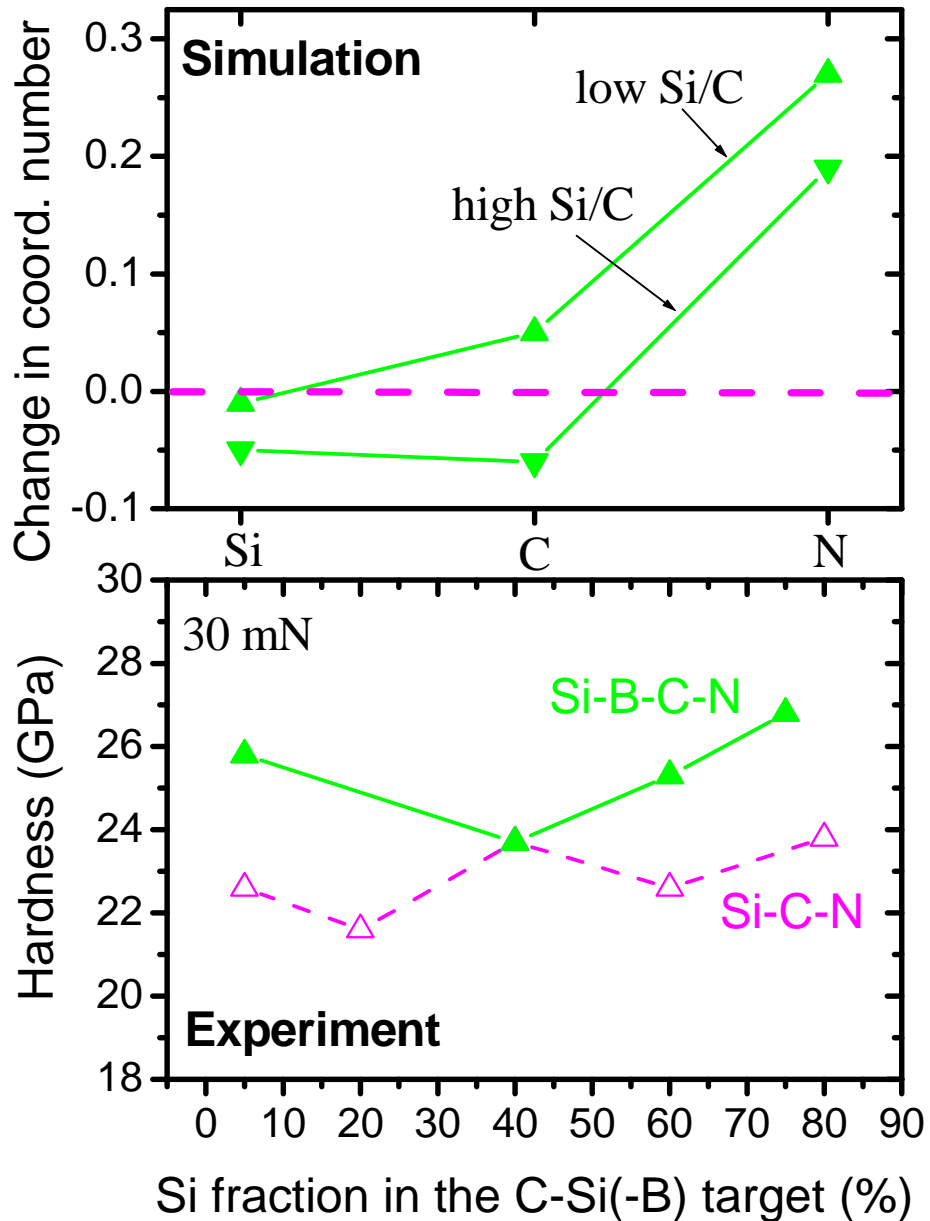
Temperature stability of Si-B-C-N materials: from bonding statistics

Simulated compositions

$\text{Si}_{32}\text{B}_{12}\text{C}_3\text{N}_{53}$ prepared in
50% N₂+50% Ar, N/(Si+B+C) = 1.13

$\text{Si}_{42}\text{B}_{11}\text{C}_2\text{N}_{45}$ prepared in
25% N₂+75% Ar, N/(Si+B+C) = 0.82

- A low abundance of less thermally stable Si-Si bonds at $\mathbf{N/(Si+B+C) > 1}$
⇒ maintenance of the amorphous state at higher temperatures



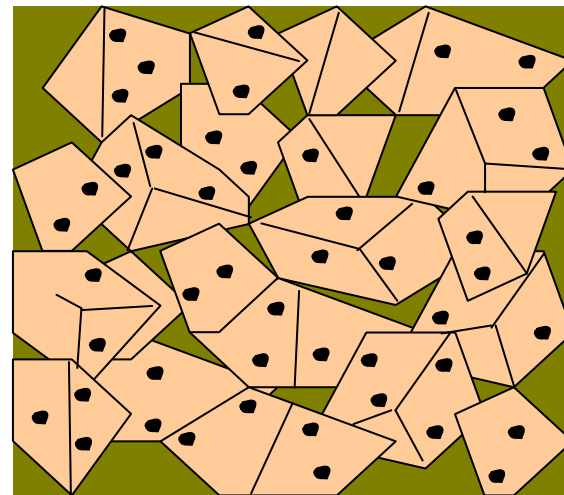
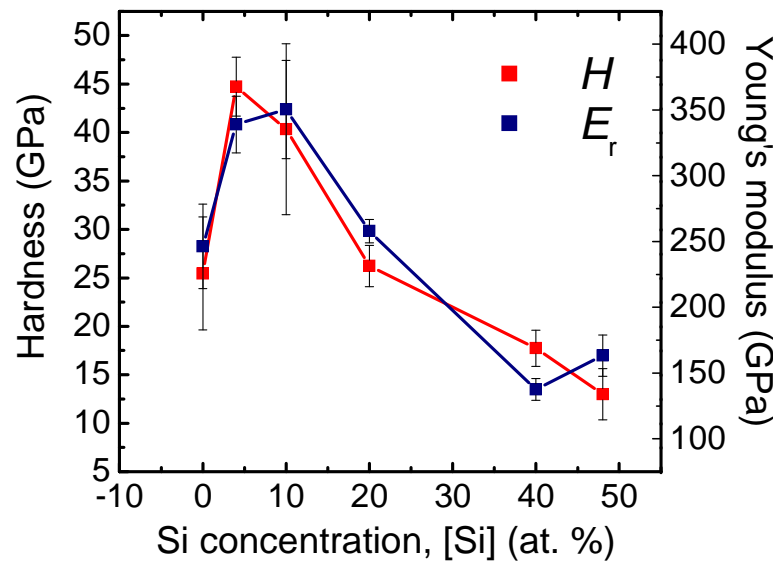
Role of B - comparing of Si-C-N and Si-B-C-N (experiment and molecular dynamics)

- Preferential bonding of B to N \Rightarrow **converting of some N lonepairs to bonding electrons** \Rightarrow higher N coordination
- Improved mechanical properties and thermal stability

2. Nanocrystalline TiSiN

	DFT (Ab-initio)	Empirical potentials
Properties	3. crystalline (Ti/Cr)N+Si,C	
Liquid- quench	1. amorphous (dense) SiBCN	2. nanocomposite TiN+SiN
Atom by atom dep.		4. amorphous (voids) SiNH

Motivation (nc-TiSiN)

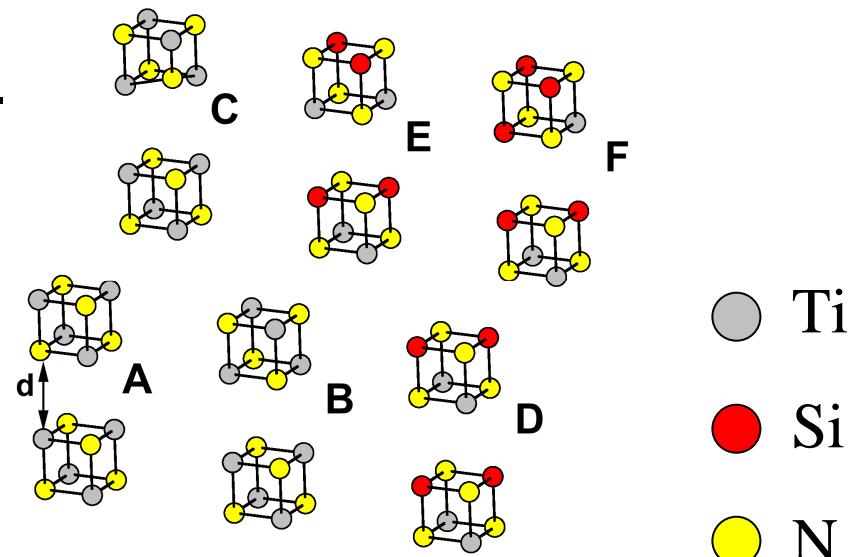


- Enhanced hardness of TiSi(C)N at $[Si] = 5\text{-}10\%$ \Leftrightarrow nanoparticles (with impurities) in an amorphous matrix
- Predict crystal size distribution, amorphous phase thickness, maximal impurities concentration, etc.

Methodology needed (nc-TiSiN)

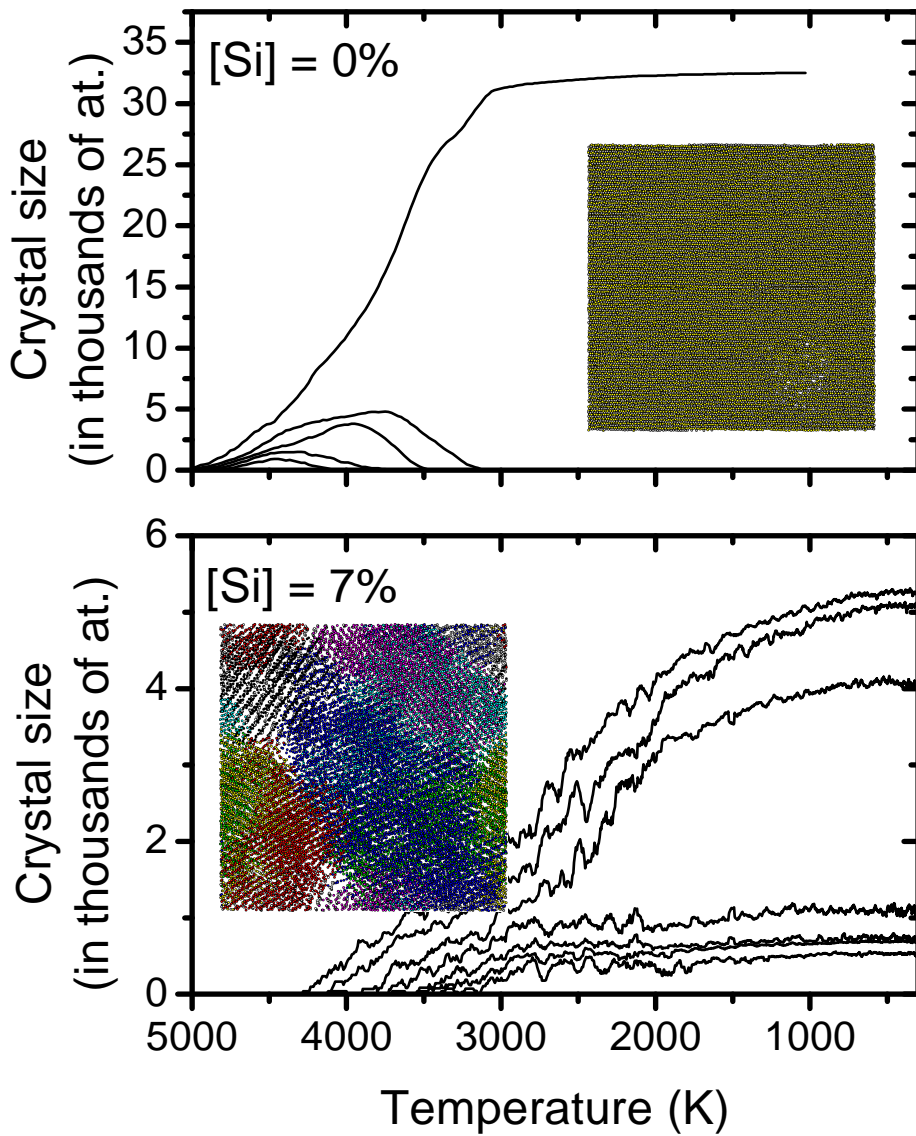
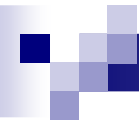
- **Empirical interaction potential**

- fitted using DFT (ab-initio) energies calculated for various fcc-Ti(Si)N configurations
- DL POLY code



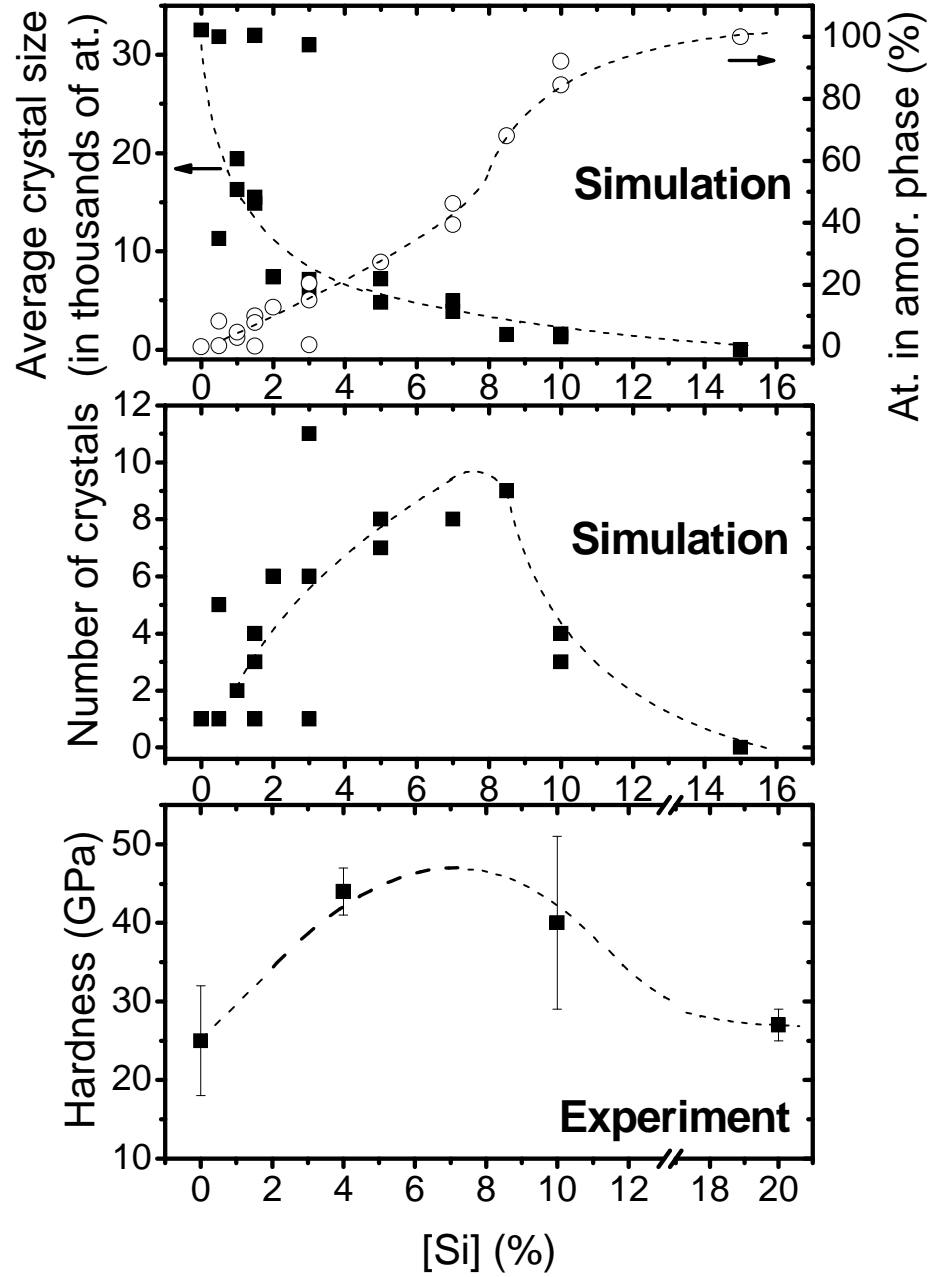
- **Molecular-dynamics simulation protocol in order to predict preferred nanocrystalline structures**

- liquid-quench as in the a-SiBCN case:
 - amorphous structures independent of the cooling time after $\sim 10^{-12}$ s
 - nanocryst. structures independent of the cooling time after $\sim 10^{-9}$ s



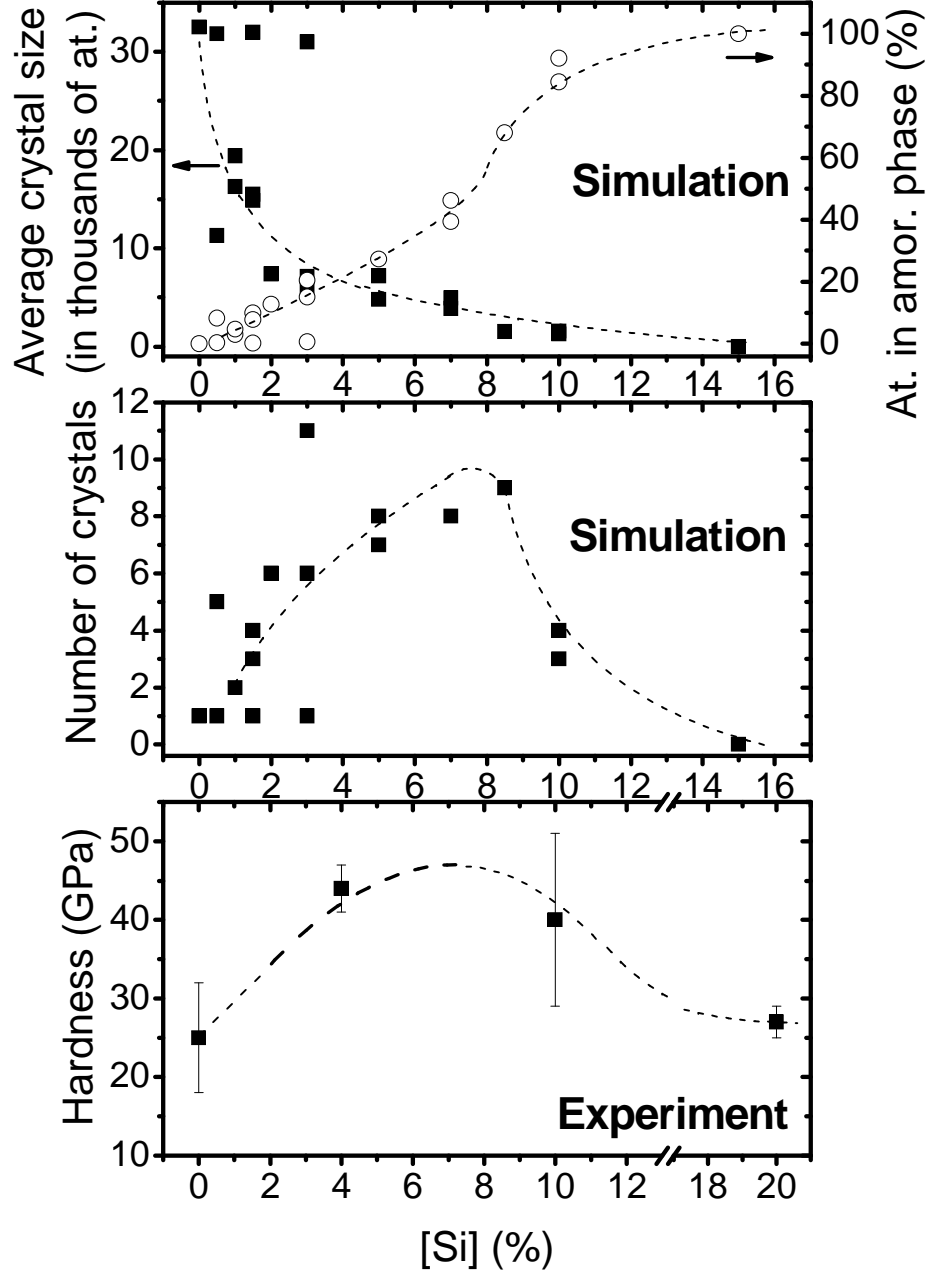
**Searching for preferred structure by exponential cool down:
dependence on [Si]**

- **0% Si:** monocrystal
(up to 8 crystals; 1 survived)
- **7% Si:** nanocomposite
(up to 10 crystals; 8 survived)



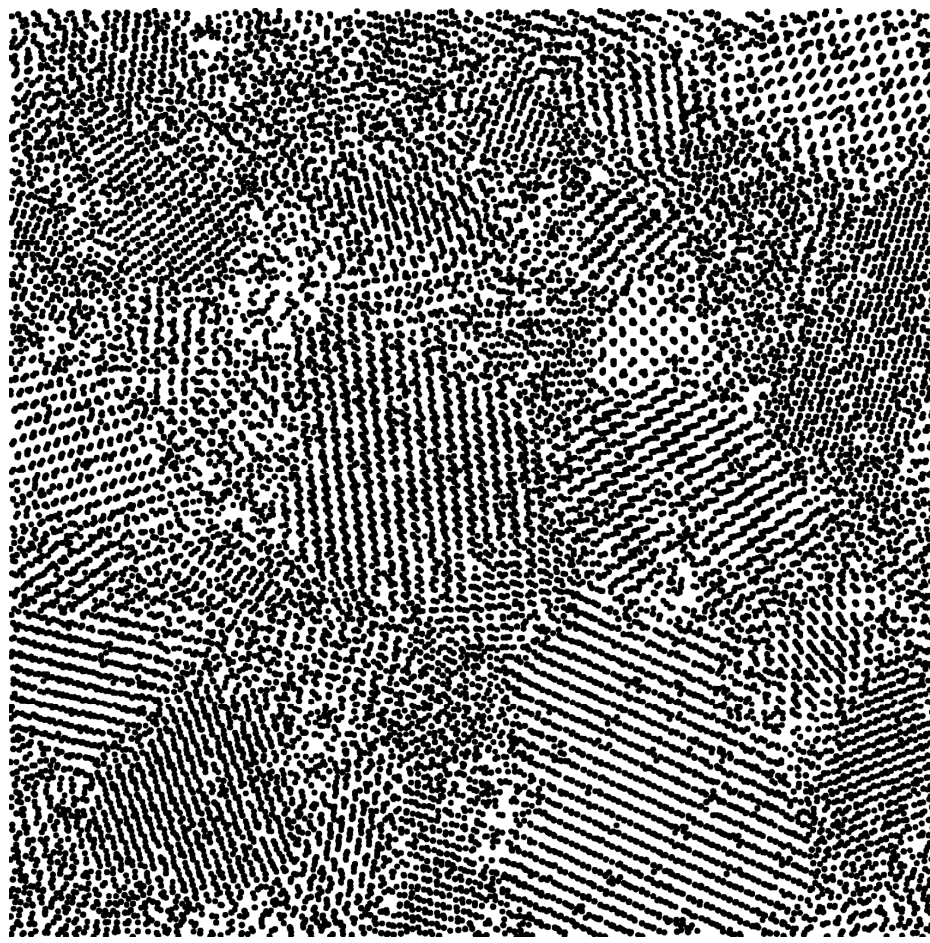
Structures formed: dependence on [Si]

- $[Si] \leq 3\%$: monocrystals
- $[Si] < 8.5\%$: increasing number of crystals, N
 - highest N : crystals of 4-7000 at. (**3-6 nm**)
- $[Si] > 8.5\%$: decreasing N
- $[Si] \geq 15\%$: amorphous
- Experiment: e.g. $\leq 4\text{-}5\text{nm}$ in S. Veprek *et al.*, *Nanostruct. Mater.* 10, 679 (1998)



Structures formed: dependence on [Si]

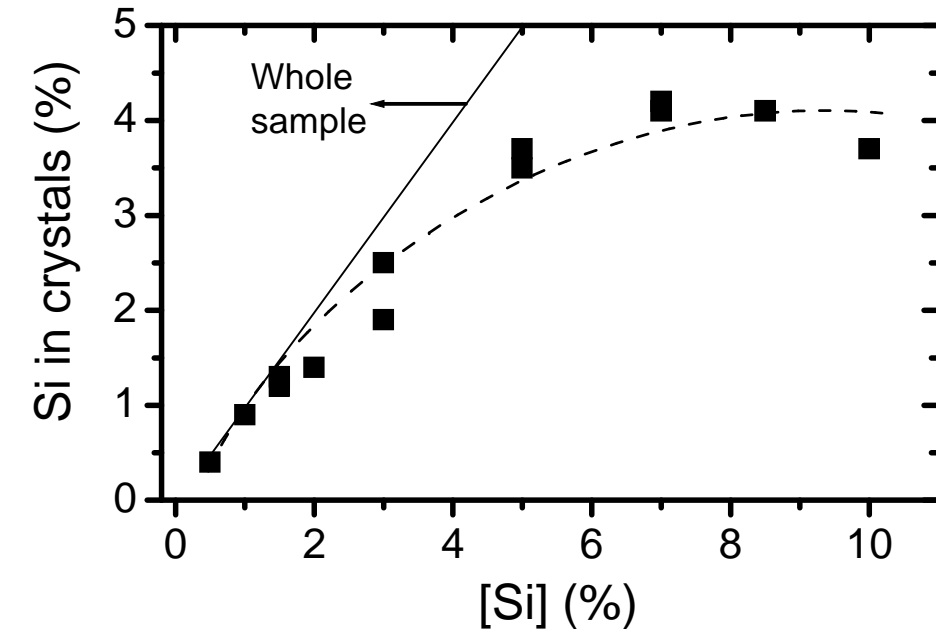
- $[Si] \leq 3\%$: monocrystals
- $[Si] < 8.5\%$: increasing number of crystals, N
highest N: crystals of 4-7000 at. (3-6 nm)
- $[Si] > 8.5\%$: decreasing N
- $[Si] \geq 15\%$: amorphous
- Experiment: e.g. **8.9%** and **15.5%** in J.H. Jeon *et al.*, *Surf. Coat. Technol.* 188, 415 (2004)



**Fine nanostructures
formed at [Si] ~ 7%:
thin slice of a final
structure**

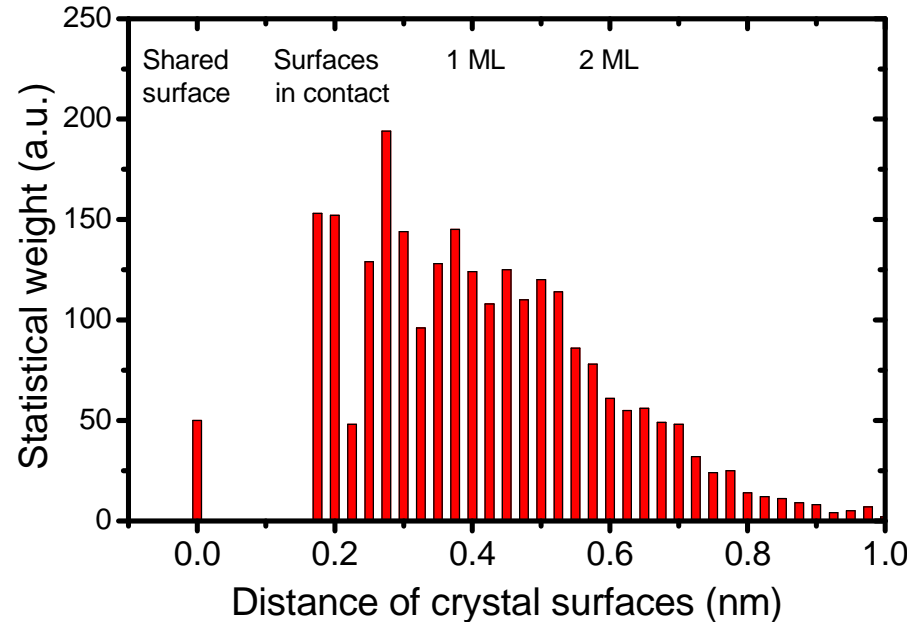
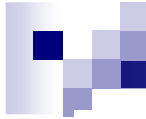
- Crystals of various orientations
- Occasionally not separated by the amorphous phase, but directly touch each other

14 nm (262.000 atoms)



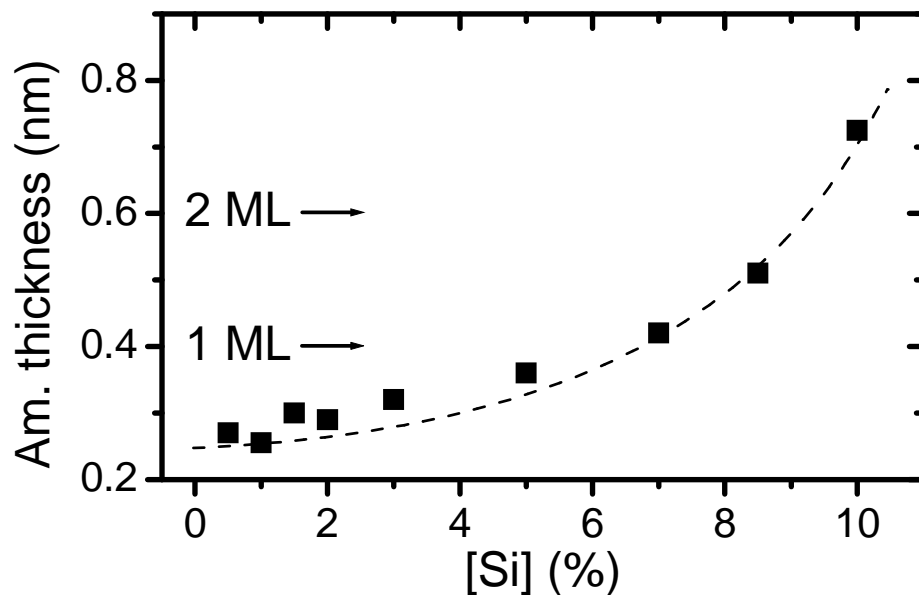
Si defects in crystals

- Up to **4%** Si trapped in TiN crystals ($\Rightarrow \text{Ti}_{0.92}\text{Si}_{0.08}\text{N}$)
- Experiment (at low mobility of atoms - low T, E_{ion}):
e.g. **4.5%** in *A. Flink et al., J. Mat. Res. 24, 2483 (2009)*



Thickness of the amorphous phase

- Distribution of distances to the nearest surface atom of another crystal



- Weighted average of the distances: **1 monolayer at [Si] = 7%**

3. Characteristics of fcc-MSiCN

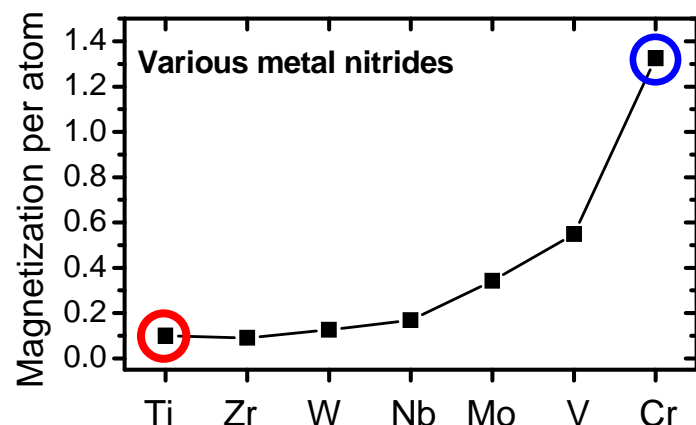
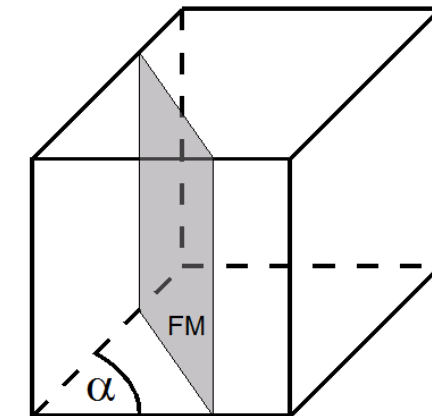
	DFT (Ab-initio)	Empirical potentials
Properties	3. crystalline (Ti/Cr)N+Si,C	
Liquid-quench	1. amorphous (dense) SiBCN	2. nanocomposite TiN+SiN
Atom by atom dep.		4. amorphous (voids) SiNH

Motivation (fcc-MSiCN)

TiN

- high hardness
 - nonmagnetic
 - metallic-like
 - cubic
- x oxidation resistance
- x magnetic
- x semiconductive
- x low-T AFM configuration
=> shear ($\alpha < 90^\circ$)

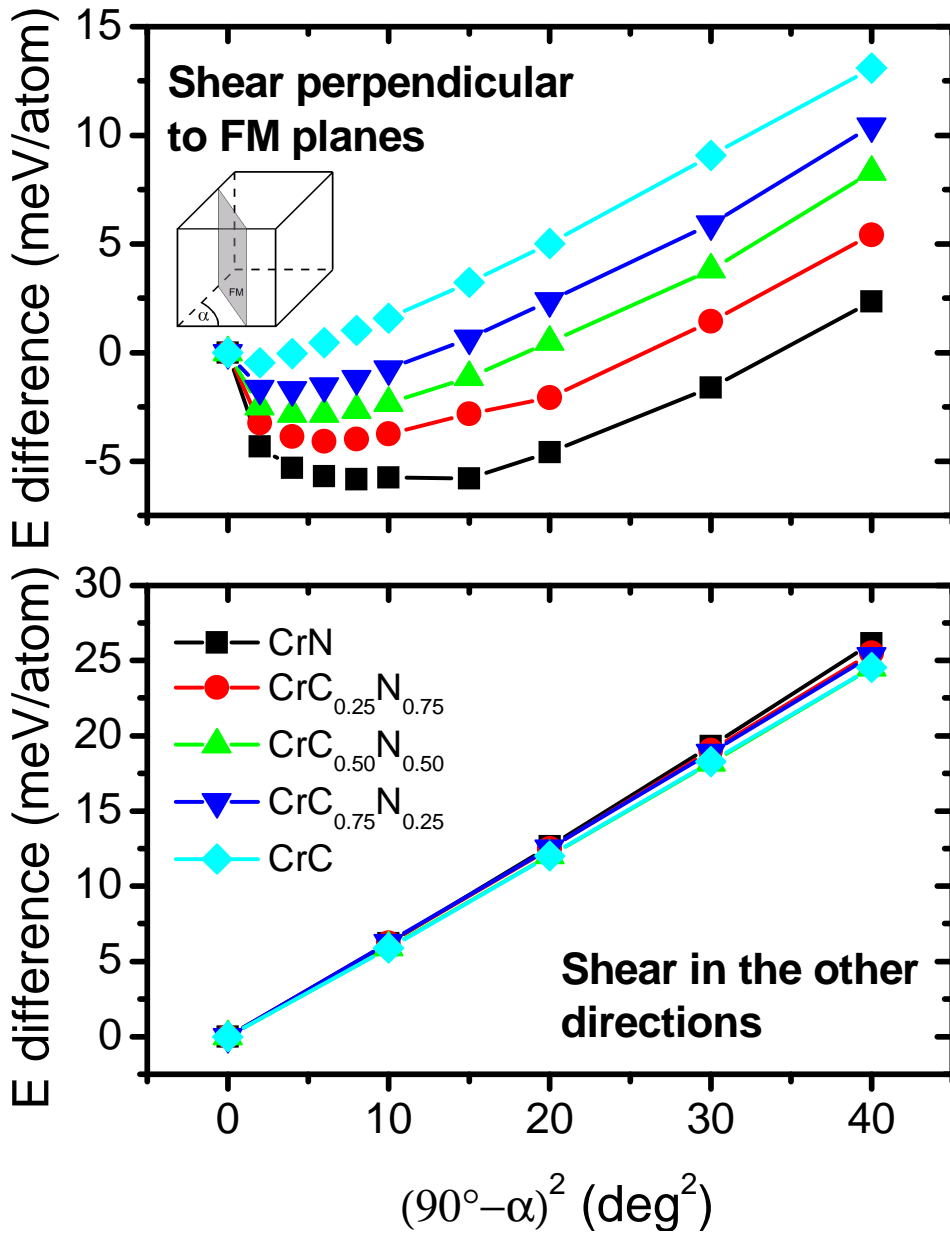
CrN



- Phenomena specific for CrN
- Different effect of Si and C in CrN and TiN

Methodology needed (fcc-MSiCN)

- **Electronic structure and energy of a crystal from given composition and deformation applied**
 - DFT: implemented in the PWSCF code
 - atom cores and inner electron shells: Vanderbilt-type pseudopotentials
 - valence electrons wavefunction: Kohn-Sham (Schrödinger-like) equations
- **Material characteristics from the energy-deformation dependencies calculated**
 - B and a_0 : by changing of cell volume
 - C_{ij} : by applying volume-conserving shear and strain
 - E, G, v for polycrystalline material: from C_{ij}



Effect of magnetization on preferred low-T structure (110 FM planes)

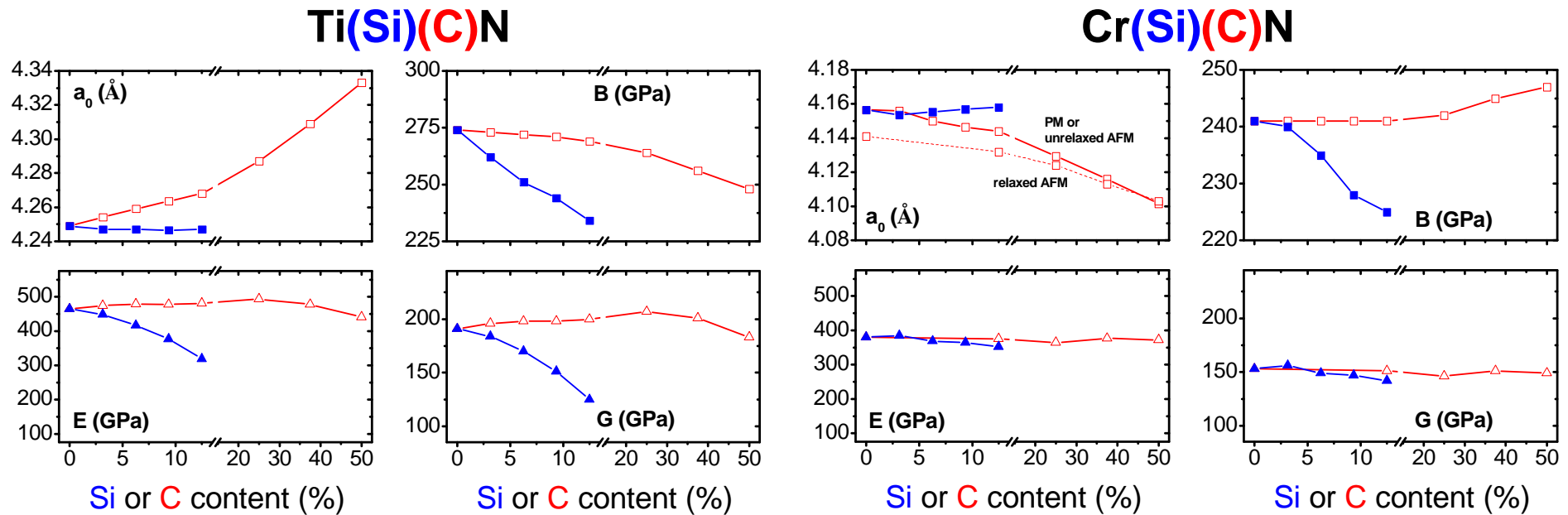
- CrN: xy shear
- C or Si addition:
(C replaces N, Si replaces Cr)
lower total mag. \Rightarrow
higher cubic preference

Characteristics of pure metal nitrides

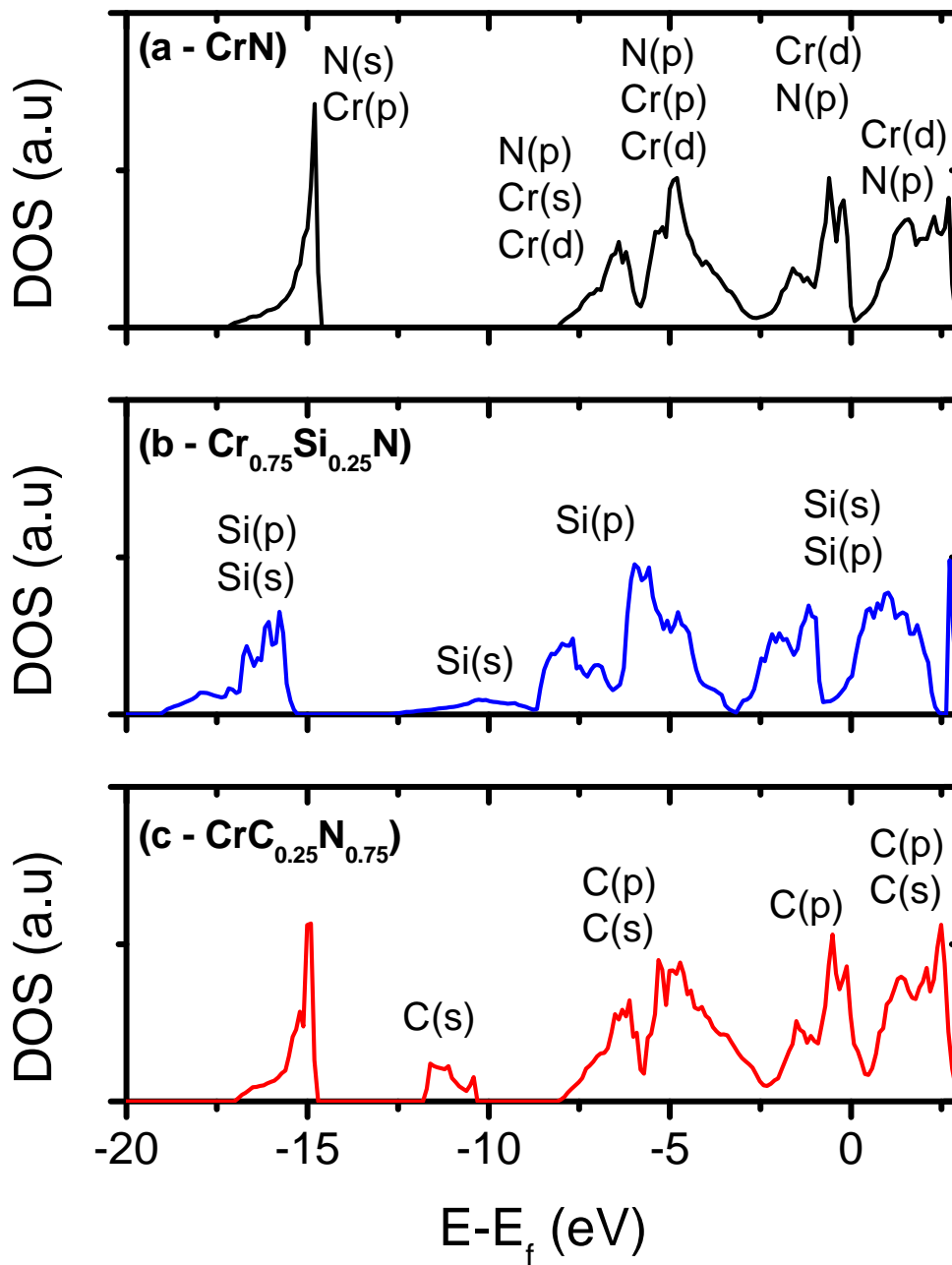
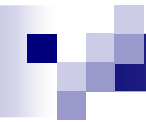
Material	Configuration	a_0 (Å)	B (GPa)	G (GPa)	E (GPa)	v
TiN	Nonmagnetic	4.249	274	191	464	0.22
CrN	Magnetic	4.156	241	153	379	0.24
CrN	Mag., relaxation of at.pos.	4.141	240	151	375	0.24
CrN	Nonmagnetic	4.050	322			

- TiN crosscheck: Agreement with previously calculated data, but large spread of experimental data especially for E
- Low-T spin ordering of CrN \Rightarrow decrease of a_0 ($4.156 \rightarrow 4.141$)
- Lower B of CrN compared to what would result from valence electron density (*magnetization penalty*)

Changes of MN characteristics: effect of C incorporation effect of Si incorporation



- Decreasing TiN moduli \propto constant / increasing CrN moduli (disappearing "magnetization penalty")
- E,G maxima for TiCN \times no extramal behavior for CrCN (shear-resistant orbitals filled for all compositions)



Density of states (DOS) for AFM CrN

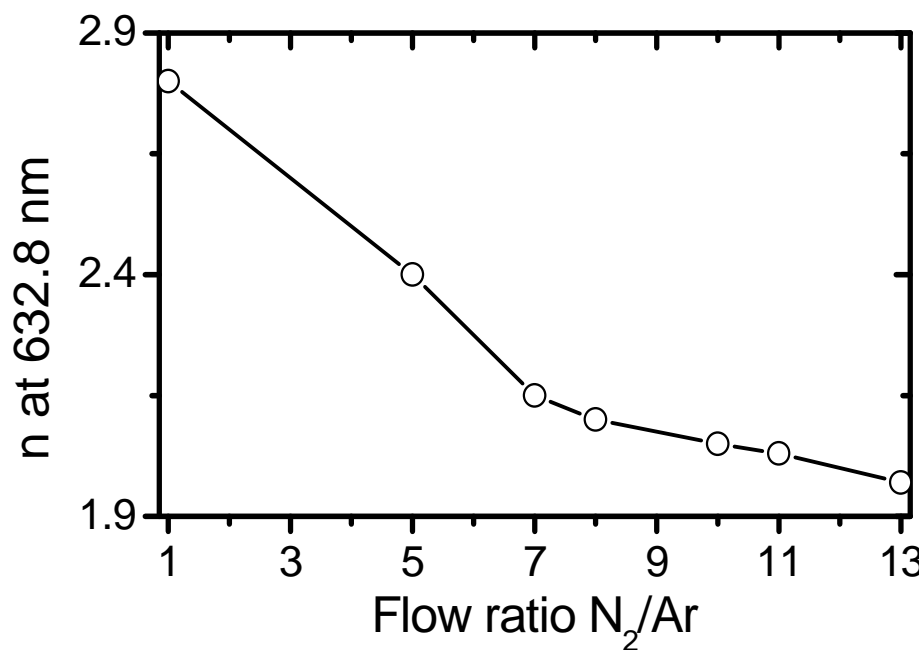
- Narrow (pseudo)gap at the Fermi energy (E_f) for pure CrN
- Si and C addition
 - ⇒ shift of the gap position
 - ⇒ the gap itself becomes less pronounced

4. Voids-containing SiNH

	DFT (Ab-initio)	Empirical potentials
Properties	3. crystalline (Ti/Cr)N+Si,C	
Liquid- quench	1. amorphous (dense) SiBCN	2. nanocomposite TiN+SiN
Atom by atom dep.		4. amorphous (voids) SiNH

Motivation (a-SiNH)

- **SiNH for single-material inhomogeneous optical filters**
(controlled fraction of voids \Rightarrow controlled n)
- **Reproduce PECVD in a mixture of SiH_4/N_2**
(main precursors: $\text{SiH}_{x \leq 3}$ and N radicals)



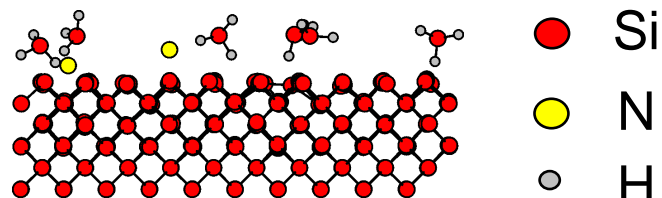
Methodology needed (a-SiNH)

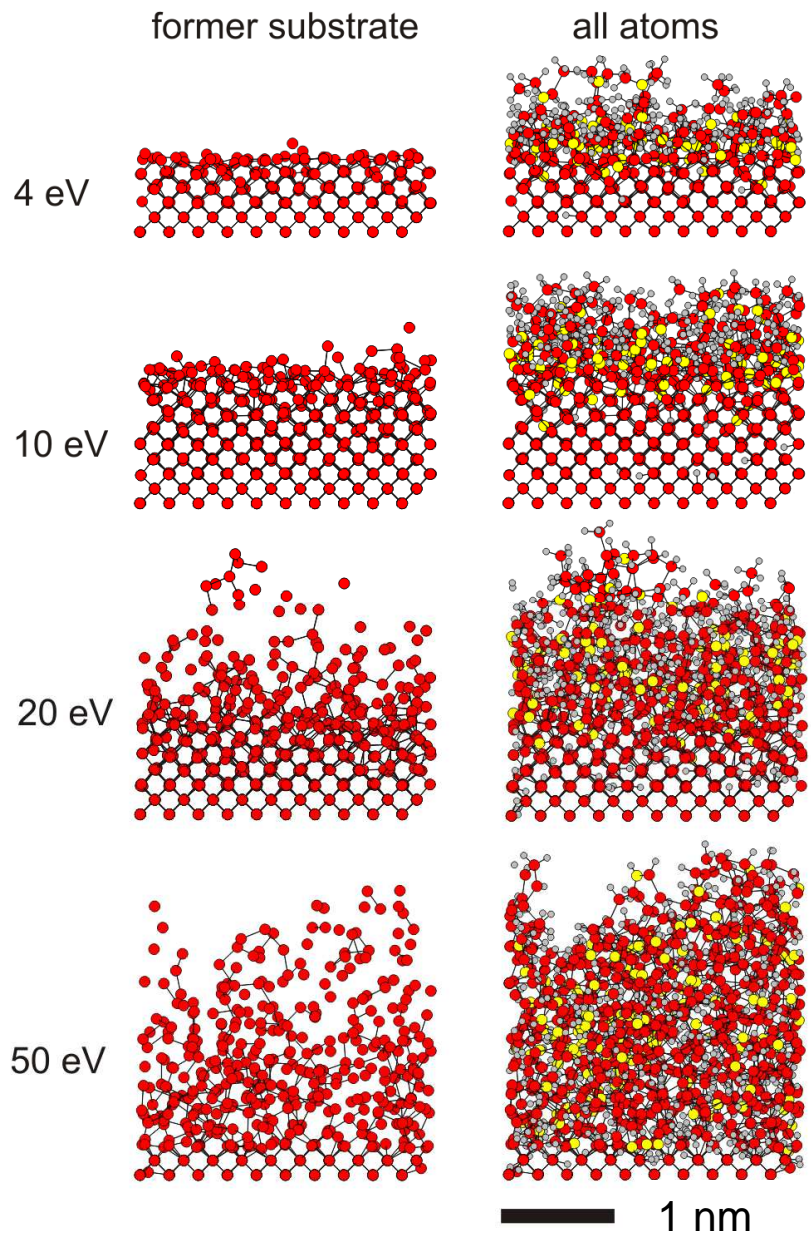
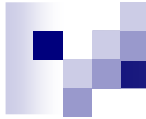
- **Empirical (Tersoff-type) interaction potential**

- atoms i,j,k and elements I,J,K: $V_{ij} = f_{ij}^{IJ} [A_{ij} \exp(-\lambda_{ij}^{IJ} r_{ij}) - b_{ij}^{IJ} B_{ij}^{IJ} \exp(-\mu_{ij}^{IJ} r_{ij})]$
dependence on distance, bonding angle, bond order (coordination numbers):
 $b_{ij}^{IJ} = f(\chi^{IJ}, \beta^I, \beta^J, n^I, n^J, c^I, c^J, d^I, d^J, h^I, h^J, r_{ik}, r_{jk}, \theta_{jik}$ over all k)

- **Recursive atom-by-atom simulation protocol**

- 1) new SiH_x and N particles (x, SiH_x/N, ion fraction F_i, ion energy E_i, flux angle)
- 2) fixed-energy run: particle collisions and energy dissipation
- 3) fixed-temperature run: reestablish the deposition T
- 4) removal of resputtered/desorbed particles

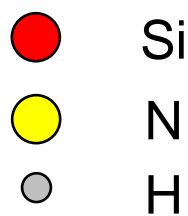


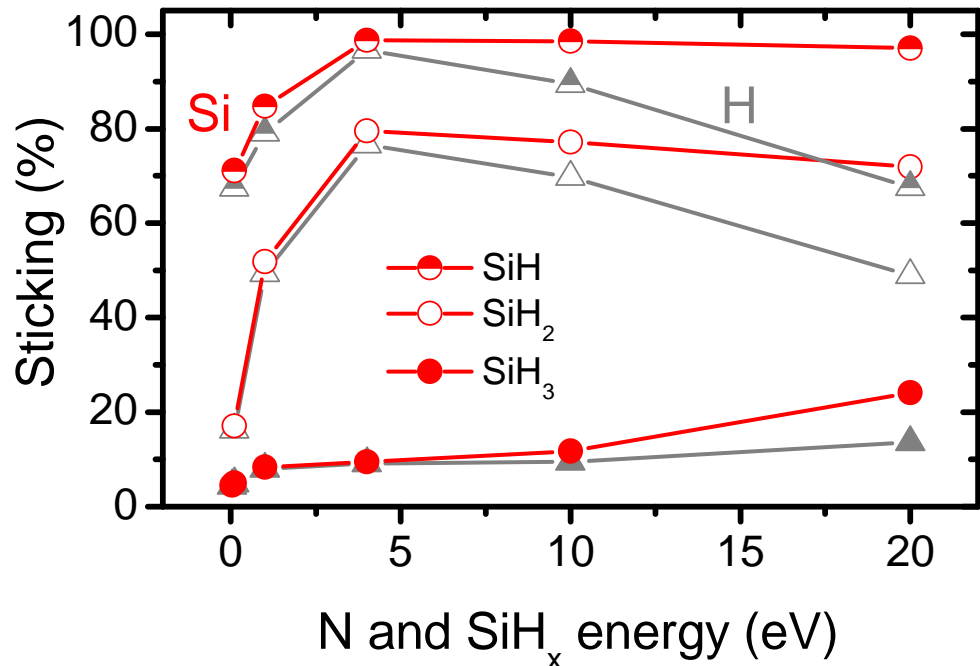
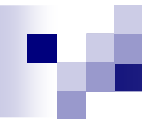


Mechanism of SiNH growth from SiH₃ and N: mixed zone formation

**Si/N deposited ratio = 52/25,
25% ion fraction**

- Surface layer of SiH₃ (dissociated by energetic particles)
- Formation of mixed zone (damage layer) on the substrate-film interface

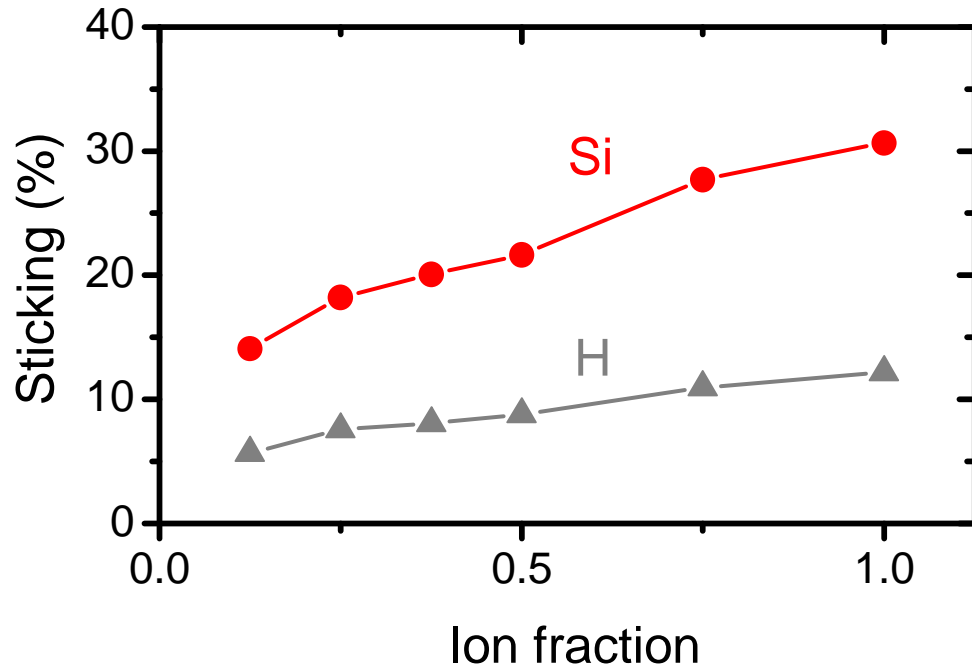
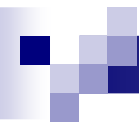




Mechanism of SiNH growth from SiH_3 and N : SiH_x dissociation

same E of all particles, 90° angle,
 Si/N deposited ratio = 52/25

- Much higher Si sticking at $x=2$ (or 1) compared to $x=3$
- H/Si ratio is lower
 - for higher energy per particle
 - if same total energy is distributed among less particles (not shown)
 - at flux angle $<90^\circ$ - only "well dissociated" SiH_3 stick (not shown)

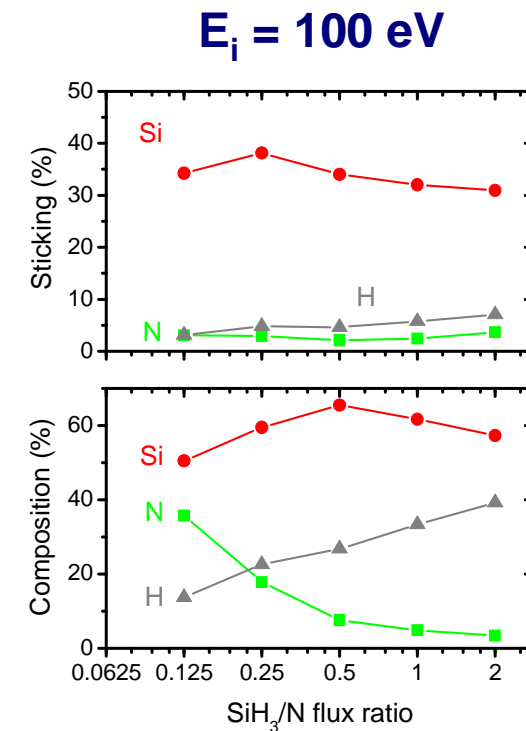
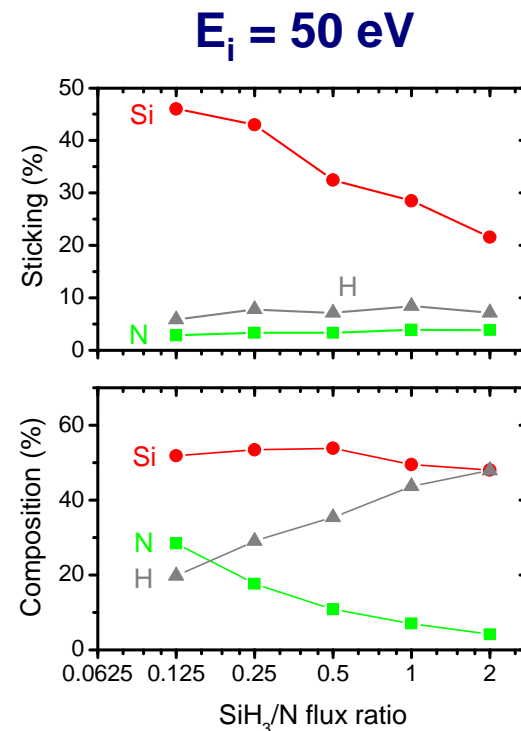
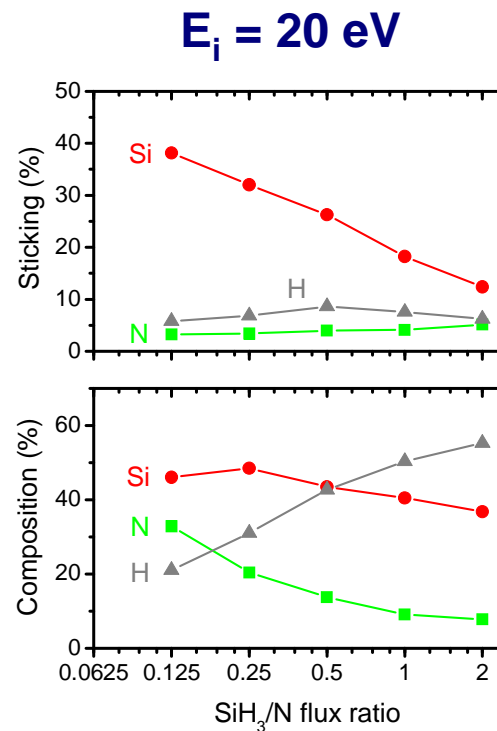


Effect of ion fraction, F_i , on dep. char.

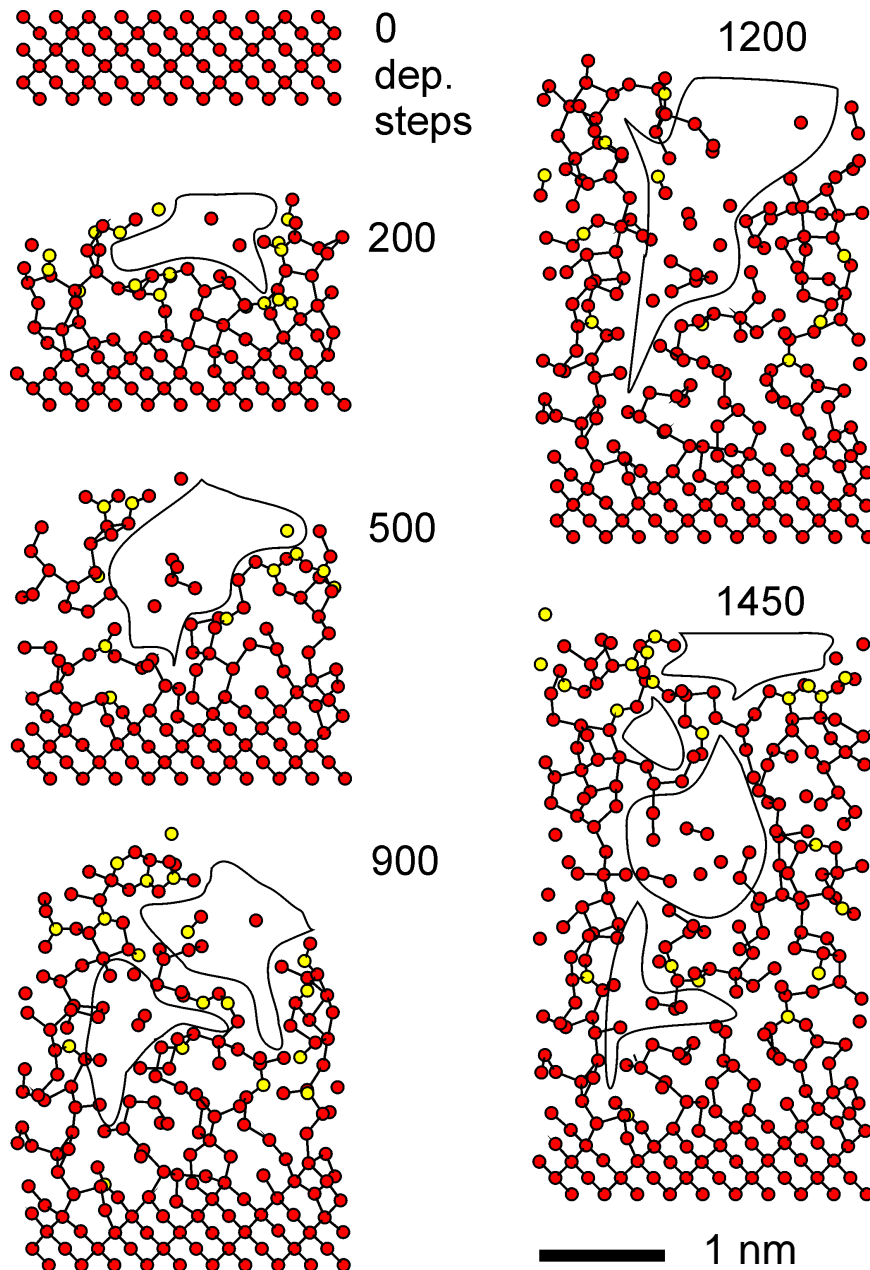
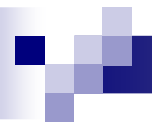
$E_i = 20 \text{ eV}$, SiH_3/N flux ratio 1/1

- Increasing $F_i \Rightarrow$ linearly increasing Si (and H) sticking coef.
- Model of "*growth from ions*": on the average, an ion dissociates the same number of SiH_3 at any F_i

Effect of E_i and flux comp. on dep. char. (ion fraction $F_i = 0.25$)



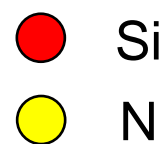
- Dependence of the Si sticking coefficient on the SiH₃ + N flux composition is more significant at lower E_i (SiH₃ is dissociated by both SiH₃⁺ and N⁺)
- H/Si ratio systematically increases with increasing SiH₃/N (H delivered only by SiH₃, but resputtered by both SiH₃⁺ and N⁺)

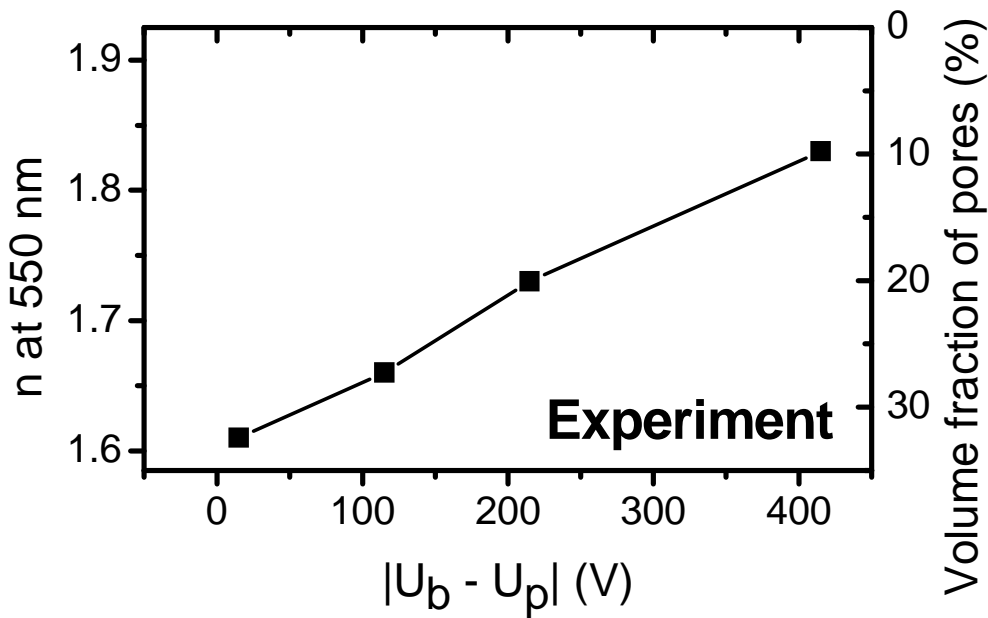
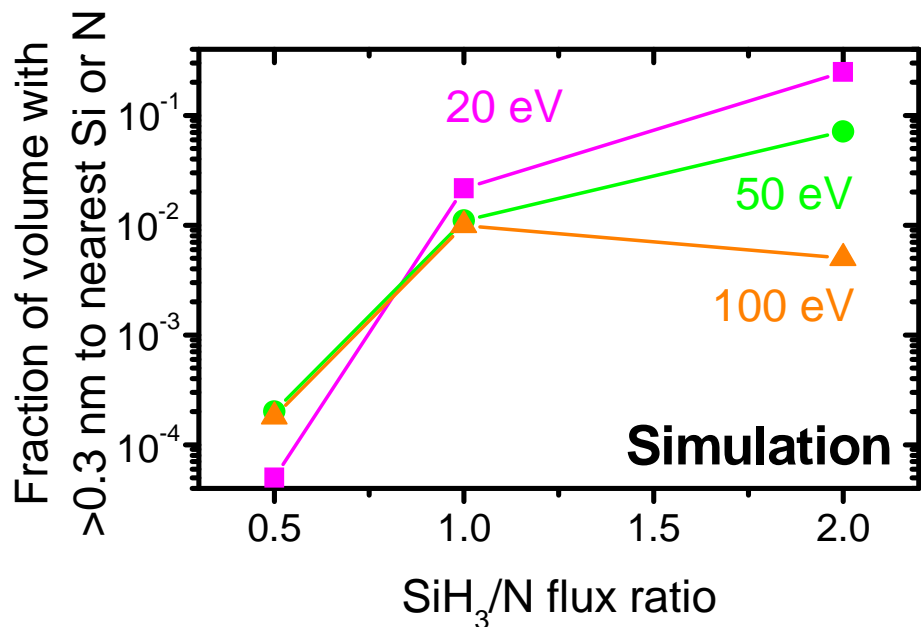
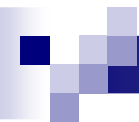


Example of growth of voids-containing SiNH

25% ion fraction, low E_i of 20 eV,
medium SiH_3/N flux ratio of 1:1

- 0.5 nm thick slices, H not shown
- 1-2 nm (non-spheric) voids





Size of voids

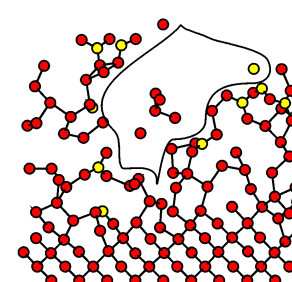
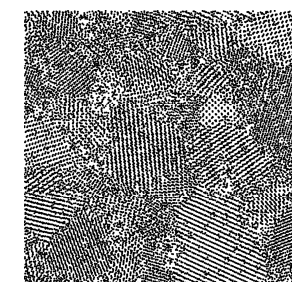
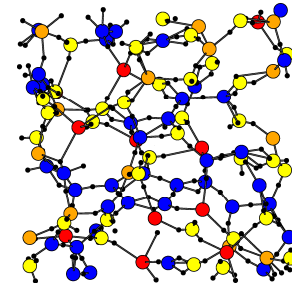
fractional volume of empty spheres with diameter > 0.6 nm

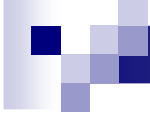
25 % ions, various E_i and flux composition

- Only lower bound of non-spheric voids size shown
- Higher voids volume for
 - lower E_i (exp. lower |U_b - U_p|)
 - higher SiH₃/N flux ratio

Conclusions (data calculated)

- Deposition characteristics
(sticking coefficients, dissociation of molecules)
- Material structures on nm scale
(distribution of crystal sizes, voids)
- Material structures on atomic scale
(bonding statistics, coordination numbers)
- Material properties
(formation E, electronic structure, band gap, magnetization)
- Temperature-dependent characteristics
(bond lifetimes, gas molecules formation)





Acknowledgements

J. Vlcek, J. Capek, P. Zeman

Department of Physics, University of West Bohemia, Czech Republic

M.M.M. Bilek, D.R. McKenzie, O. Warschkow

School of Physics, University of Sydney, Australia

L. Martinu, J.E. Klemburg-Sapieha

Department of Engineering Physics, Ecole Polytechnique Montreal, Canada

MSM 235200002, MSM 4977751302, Australian

Partnership for Advanced Computing, Australian Centre
for Advanced Computing and Communications,
Metacentrum Czech Republic, RQCHP of Quebec